IIETA International Information and Engineering Technology Association
Advancing the World of Information and Engineering

Mathematical Modelling of Engineering Problems
Vol. 11, No. 10, October, 2024, pp. 2740-2748
Journal homepage: http://iieta.org/journals/mmep

Weibull Statistic in Hydrolytic Aging of Polyesterimide Used in Rotating Electrical Machine Windings

Mohammed Nedjar*, Fatima Kerkarine

Laboratoire de Génie Electrique, Université Mouloud Mammeri, Tizi-Ouzou 15000, Algeria

Corresponding Author Email: mohammed.nedjar@ummto.dz

Copyright: ©2024 The authors. This article is published by IIETA and is licensed under the CC BY 4.0 license (http://creativecommons.org/licenses/by/4.0/).

https://doi.org/10.18280/mmep.111016

Received: 30 March 2024
Revised: 15 August 2024
Accepted: 30 August 2024
Available online: 31 October 2024

Keywords:
polyesterimide, moisture, aging, breakdown voltage, electrical machines, statistics, FTIR, degradation

ABSTRACT

This study treats the effect of hydrolytic aging on breakdown voltage of polyesterimide employed in rotating electrical machine windings. The aging was carried out at 93% relative humidity and 40°C in a climatic chamber. The samples were made as twisted pair copper conductors covered by a thin layer (35 µm) of polyesterimide. The duration of aging is 12000 h (500 days). The values of breakdown voltage were analyzed statistically using Weibull model. The insulation was characterised by FTIR. The study shows modifications of breakdown voltage versus aging time. The decrease is attributed to the increase in free volume leading to the raise in mean free path of charge carriers. While the raise is awarded to the arrangement of the structure. The shape parameter of Weibull plots alters versus aging time. The shortening is attributed to the raise of defect sizes. Whereas the augmentation is allotted to the arrangement of molecular structure. During the tests of dielectric failure, space charge can be formed and affect breakdown voltage. The results of FTIR show the disappearance of several absorbance peaks highlighting the degradation of the material. The degradation is done by the decomposition of imide bond and ester bond at the polyesterimide-copper interface.

1. INTRODUCTION

Farahani et al. [1] reported that the electrical insulation system of high voltage rotating machines is one of the most important parts of them in function of the making cost as well as to the maintenance and the lifetime aspects.

Polyesterimide, polyamide imide, and polyimide are widely utilized in windings of rotating electrical machines. For their selection, it is necessary to considerer various factors: working environment, applied voltage, rotating rate, and operating temperature. Kavanagh et al. [2], and Grubic et al. [3] yielded that the degradation of insulation materials is a major failure mode of electromagnetic coils and electrical machines.

Ksouri et al. [4] considered the water absorption in polyamide 6 (PA6) and polyamide 6 reinforced with 30% of glass fibers (PA6GF30) in distilled water at 90°C for 80 days. The humidity contents are 8.55 wt% and 5.26 wt% for PA6 and PA6GF30, respectively.

During the operation of electrical machines, the insulation is submitted to the action of moisture. Ji et al. [5] investigated the effect of combined moisture-temperature on partial discharges of copper wires insulated with polyesterimide (class H). The twisted pair specimens were exposed to relative moisture ranging from 30% to 90% at different temperatures: 30°C, 60°C and 90°C. To evaluate performance of the polymeric material, dielectric loss factor (tgδ), and insulation capacitance (IC) were measured. AC voltage, 50 Hz was applied to the samples with a rate of 700V/s. The authors concluded that tgδ and IC increase with relative humidity. A variation of partial discharge inception voltage versus relative humidity was indicated.

Brandes et al. [6] studied the insulation resistance of polyesterimide mica under hydrolytic aging. Samples were immerged in water. The authors noticed an exceptional resistance to water penetration of the dielectric material after 40 days of aging.

Because of its good properties as dielectric parameters, polyesterimide plays a major role in the field of electrical insulation as mentioned by Arikan et al. [7], and Havran et al. [8]. Despite of its high performance, investigations highlighted degradation of the material under moisture [9, 10]. Lian et al. [9] exhibited samples of polyesterimide to hydrothermal aging. The specimens were aged in oven at 80°C and 100% relative humidity. The investigation pointed that the glass transition temperature reduces from 333 K to 326 K after 30 days of aging. Niu et al. [10] studied the effect of hydrothermal aging on breakdown strength of polyesterimide. The specimens were exposed in oven regulated at 80°C and 100% relative humidity during 14 days. The breakdown test was conducted under AC voltage, 50 Hz. The voltage was evenly raised with a speed of 2 kV/s. The investigation indicates a decrease of dielectric strength from 67.27 kV/mm to 32.11 kV/mm after 14 days of aging. The moisture absorptions are 1.50wt% and 1.62wt% after 7 days and 14 days, respectively.

This work reported the investigation of breakdown voltage of polyesterimide under hydrolytic aging. A statistical study of breakdown voltage data was achieved using the Weibull model. The insulation was characterised by Fournier Transform Infrared Spectroscopy (FTIR).

2. EXPERIMENTAL METHODS

2.1 Specimens

A bobbin of copper wire enameled with polyesterimide was furnished by TREFICUIVRE, manufacturer in ALGERIA. The insulation, of class H (180°C), has a 35 µm coat. The diameter of the wire is 0.63 mm.

The samples were prepared as twisted pair conductors. Firstly, the insulated wire was cut into lengths of 400 mm. The samples were elaborated using a winding lathe. A weight of 7 N was hooked to the wire, then 12 turns were carried out. At the end, the weight was detached and the buckle located at the top part of the specimen was suppressed. The length of the realized samples is 125 mm. To avert bypasses during the test of dielectric failure, the extremities of the samples were separated. In order to avoid any attendance of defects, the specimens were inspected with a microscope. Figure 1 illustrates a performed sample.

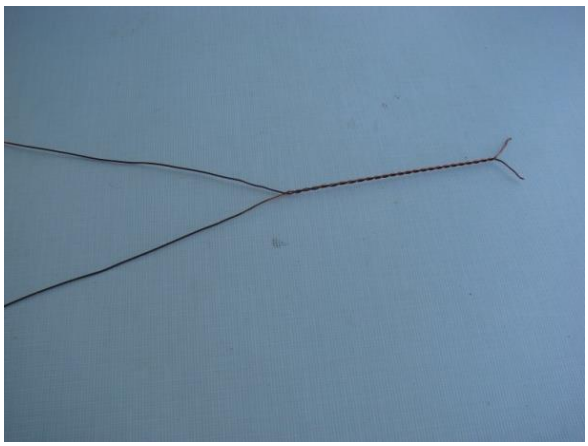

Figure 1. Photograph of an achieved specimen

2.2 Hydrolytic aging

A great number of samples was exhibited to moisture in a climatic chamber regulated at 93% relative humidity and 40°C. The aging was performed up to 12000 h (500 days). To obtain this humidity level, 1.215l of glycerin was mixed with 6.075l of distilled water. The glycerin volume represents 20% of that of distilled water. The enclosure is equipped by temperature regulator and a heating system. After each period of 500 h, 80 specimens were withdrawn from the climatic chamber.

2.3 Dielectric breakdown test

AC voltage, 50 Hz provided by a high voltage transformer, was applied to the extremities of the twists. The voltage was raised with a speed of 0.5 kV/s until a failure occurred. The breakdown voltage was registered. The experiments were executed in air and at ambient temperature. A number of 2000 specimens was tested.

2.4 Fournier Transform Infrared Spectroscopy

For the tests of FTIR, a powder of the polymer was mixed with a KBr amount. After blending, the whole was pressed, then the pellets were made. The infrared spectra were measured with JASCO FT/IR in the wavenumber range of 4000 - 500 cm^{-1}. The apparatus is equipped with a computer.

3. STATISTICAL ANALYSIS OF BREAKDOWN VOLTAGE DATA

It is well known that failure is a random phenomenon and a statistical study of breakdown voltage or time-to-rupture is useful. Weibull model is widely employed in the investigation in dielectric breakdown of solid dielectrics [10, 11]. A detailed description of this model can be found in a reference book [12]. The two-parameter Weibull distribution is given by Chauvet and Laurent [13]:

$$P(V) = 1 - exp\left[-\left(\frac{V}{V_o}\right)^{\beta}\right] \quad (1)$$

where:

$P(V)$: cumulative breakdown probability;

V: breakdown voltage;

V_0: scale parameter that is the value of V matching to a cumulative probability of 63.2%;

β: shape parameter which is the slope of the straight line of Weibull plot.

The precedent relationship can be written as below:

$\log\mathrm{Ln}\frac{1}{1-P} = \beta\log V - \beta\log V_o$ with P(V) = P.

In the coordinate system $X = \log V$ and $Y = \log\mathrm{Ln}\frac{1}{1-P}$, the plot must be a straight line. For $V = V_o$, $\log\mathrm{Ln}\frac{1}{1-P} = 0$ and $P = 1 - \frac{1}{e} = 63.2\%$.

The statistical study was executed following the steps underneath:

1. The rank i of each value of V was determined according to a classification by ascending order.
2. The cumulative breakdown probability P was evaluated, for each value of breakdown voltage utilizing the formula at the bottom [14]:

$$P = \frac{i}{N + 1}\ 100\% \quad (2)$$

where:

N: total number of tested specimens; in this work $N = 80$.

3. Calculation of $X = \log V$ and $Y = \log\mathrm{Ln}\frac{1}{1-P}$.
4. Representation of the dots giving $\log\mathrm{Ln}\frac{1}{1-P}$ versus $\log V$.
5. The best linear fit of Weibull plot was established by an estimation based on the method of the maximum likelihood.
6. Calculation of the 90% confidence intervals. We considered different percentiles: 1%, 5%, 10%, 15%, 20%, 25%, 30%, 35%, 40%, 45%, 50%, 55%, 60%, 63.2%, 70%, 75%, 80%, 85%, 90%, 95% and 99%. The confidence bounds were computed using the maximum likelihood method.
7. Plot of the confidence intervals.
8. The values of V_0 and β were deducted. All the calculations were executed with a computer program established by "Laboratoire de Génie Electrique de Toulouse, France", nowadays "LAPLACE".

4. RESULTS AND DISCUSSION

4.1 Statistical analysis

a) Table 1(a) depicts the values of V, P, X and Y before

aging. The findings of confidence intervals of breakdown voltage are presented in Table 1(b). For 12000 h of aging, the results of V, P, X and Y, and confidence bounds are exposed in Tables 2(a) and 2(b), respectively.

Table 1(a). Values of V, P, X and Y before aging

No.	V (kV)	P	X	Y
1	9.2	0.1975	0.9638	- 0.6575
2	10.6	0.4198	1.0253	- 0.2642
3	14.1	0.9877	1.1492	0.6429
4	12.3	0.7531	1.0899	0.1457
5	10.7	0.4444	1.0294	- 0.2308
6	10.9	0.5062	1.0374	- 0.1515
7	12.0	0.6914	1.0792	0.0702
8	9.8	0.3210	0.9912	- 0.4122
9	11.5	0.6173	1.0607	- 0.0175
10	9.5	0.2716	0.9777	- 0.4991
11	9.4	0.2469	0.9731	- 0.5473
12	11.1	0.5679	1.0453	- 0.0762
13	11.1	0.5679	1.0453	- 0.0762
14	9.8	0.3210	0.9912	- 0.4122
15	11.6	0.6296	1.0645	- 0.0029
16	9.4	0.2469	0.9731	- 0.5473
17	12.9	0.8765	1.1106	0.3205
18	7.0	0.0247	0.8451	- 1.6020
19	12.9	0.8765	1.1106	0.3205
20	11.9	0.6543	1.0755	0.0262
21	12.5	0.7901	1.0969	0.1935
22	11.4	0.5802	1.0569	- 0.0614
23	7.9	0.0741	0.8976	- 1.1137
24	13.3	0.9383	1.1239	0.4448
25	9.6	0.2840	0.9823	- 0.4762
26	12.9	0.8765	1.1106	0.3205
27	13.0	0.9012	1.1139	0.3646
28	10.6	0.4198	1.0253	- 0.2642
29	12.6	0.8272	1.1004	0.2444
30	9.8	0.3210	0.9912	- 0.4122
31	13.5	0.9506	1.1303	0.4783
32	12.3	0.7531	1.0899	0.1457
33	8.8	0.1481	0.9445	- 0.7950
34	11.0	0.5309	1.0414	- 0.1210
35	9.1	0.1852	0.9590	- 0.6887
36	9.9	0.3333	0.9956	- 0.3920
37	8.1	0.1111	0.9085	- 0.9289
38	9.1	0.1852	0.9590	- 0.6887
39	10.7	0.4444	1.0294	- 0.2308
40	11.8	0.6420	1.0719	0.0116
41	12.6	0.8272	1.1004	0.2444
42	12.5	0.7901	1.0969	0.1935
43	9.3	0.2222	0.9685	- 0.5998
44	7.1	0.0370	0.8513	- 1.4232
45	13.7	0.9753	1.1367	0.5684
46	8.6	0.1358	0.9345	- 0.8358
47	12.0	0.6914	1.0792	0.0702
48	10.5	0.3704	1.0212	- 0.3348
49	11.1	0.5679	1.0453	- 0.0762
50	10.0	0.3457	1.0000	- 0.3725
51	12.8	0.8395	1.1072	0.2623
52	13.1	0.9259	1.1173	0.4154
53	12.6	0.8272	1.1004	0.2444
54	10.9	0.5062	1.0374	- 0.1515
55	11.0	0.5309	1.0414	- 0.1210
56	10.8	0.4691	1.0334	- 0.1984
57	8.1	0.1111	0.9085	- 0.9289
58	13.7	0.9753	1.1367	0.5684
59	6.8	0.0123	0.8325	- 1.9058
60	10.2	0.3580	1.0086	- 0.3534
61	9.3	0.2222	0.9685	- 0.5998
62	7.6	0.0617	0.8808	- 1.1958
63	10.6	0.4198	1.0253	- 0.2642
64	10.8	0.4691	1.0334	- 0.1984
65	8.0	0.0864	0.9031	- 1.0439
66	13.1	0.9259	1.1173	0.4154
67	12.0	0.6914	1.0792	0.0702
68	12.2	0.7284	1.0864	0.1151
69	13.0	0.9012	1.1139	0.3646
70	12.2	0.7284	1.0864	0.1151
71	11.5	0.6173	1.0607	- 0.0175
72	11.5	0.6173	1.0607	- 0.0175
73	10.9	0.5062	1.0374	- 0.1515
74	7.3	0.0494	0.8633	- 1.2955
75	9.5	0.2716	0.9777	- 0.4991
76	8.9	0.1605	0.9494	- 0.7571
77	12.5	0.7901	1.0969	0.1935
78	12.2	0.7284	1.0864	0.1151
79	10.6	0.4198	1.0253	- 0.2642
80	8.6	0.1358	0.9345	- 0.8358

Table 1(b). Confidence intervals of breakdown voltage before aging

$\log \mathrm{Ln}\frac{1}{1-P}$	Log V_{inf}	Log V_{sup}
-1.9978	0.7254	0.8223
-1.2899	0.8417	0.9088
-0.9773	0.8928	0.9475
-0.7891	0.9239	0.9705
-0.6514	0.9462	0.9880
-0.5411	0.9640	1.0019
-0.4477	0.9790	1.0133
-0.3657	0.9918	1.0238
-0.2917	1.0032	1.0337
-0.2334	1.0145	1.0422
-0.1592	1.0244	1.0507
-0.0977	1.0337	1.0591
-0.0380	1.0428	1.0668
00.00	1.0483	1.0721
0.0806	1.0603	1.0833
0.1419	1.0692	1.0920
0.2067	1.0786	1.1018
0.2781	1.0885	1.1121
0.3622	1.1001	1.1251
0.4765	1.1155	1.1423
0.6632	1.1401	1.1716

Table 2(a). Values of V, P, X and Y after 12000 h of aging

No.	V (kV)	P	X	Y
1	8.9	0.4691	0.9494	-0.1984
2	11.3	0.9259	1.0531	0.4154
3	6.1	0.0741	0.7853	-1.1137
4	10.2	0.8148	1.0086	0.2270
5	9.2	05309	0.9638	-0.1210
6	10.0	0.7654	1.0000	0.1614
7	5.3	0.0123	0.7243	-1.9058
8	10.1	0.7901	1.0043	0.1935
9	11.3	0.9259	1.0531	0.4154
10	9.8	0.7037	0.9912	0.0851
11	11.3	0.9259	1.0531	0.4154
12	6.8	0.1728	0.8325	-0.7218
13	10.1	0.7901	1.0043	0.1935
14	12.5	0.9753	1.0969	0.5684
15	7.8	0.3457	0.8921	-0.3725
16	10.9	0.8519	1.0374	0.2809
17	12.2	0.9630	1.0864	0.5180
18	10.0	0.7654	1.0000	0.1614
19	9.8	0.7037	0.9912	0.0851
20	5.6	0.0370	0.7482	-1.4232
21	9.1	0.4815	0.9590	-0.1826
22	9.3	0.5679	0.9685	-0.0762

23	7.6	0.2963	0.8808	-0.4542
24	6.9	0.1852	0.8388	-0.6887
25	7.1	0.1975	0.8513	-0.6575
26	8.7	0.4198	0.9395	-0.2642
27	8.4	0.3951	0.9243	-0.2988
28	8.5	0.4074	0.9294	-0.2813
29	11.0	0.8889	1.0414	0.3419
30	7.3	0.2346	0.8633	-0.5730
31	9.4	0.5926	0.9731	-0.0468
32	13.4	0.9877	1.1271	0.6429
33	7.8	0.3457	0.8921	-0.3725
34	10.7	0.8272	1.0294	0.2444
35	7.8	0.3457	0.8921	-0.3725
36	7.5	0.2593	0.8751	-0.5227
37	8.9	0.4691	0.9494	-0.1984
38	9.2	0.5309	0.9638	-0.1210
39	8.2	0.3704	0.9138	-0.3348
40	6.7	0.1481	0.8261	- 0.7950
41	11.0	0.8889	1.0414	0.3419
42	8.8	0.4321	0.9445	-0.2473
43	7.8	0.3457	0.8921	-0.3725
44	7.3	0.2346	0.8633	-0.5730
45	10.2	0.8148	1.0086	0.2270
46	6.4	0.1111	0.8062	- 0.9289
47	9.9	0.7407	0.9956	0.1303
48	9.5	0.6420	0.9777	0.0116
49	9.3	0.5679	0.9685	-0.0762
50	7.6	0.2963	0.8808	-0.4542
51	9.2	0.5309	0.9638	-0.1210
52	6.1	0.0741	0.7853	-1.1137
53	6.7	0.1481	0.8261	-0.7950
54	7.3	0.2346	0.8633	-0.5730
55	9.5	0.6420	0.9777	0.0116
56	9.9	0.7407	0.9956	0.1303
57	8.9	0.4691	0.9494	-0.1984
58	6.8	0.1728	0.8325	-0.7218
59	11.0	0.8889	1.0414	0.3419
60	7.6	0.2963	0.8808	-0.4542
61	10.9	0.8519	1.0374	0.2809
62	5.4	0.0247	0.7324	-1.6020
63	8.4	0.3951	0.9243	-0.2988
64	8.2	0.3704	0.9138	-0.3348
65	6.0	0.0494	0.7782	-1.2955
66	9.4	0.5926	0.9731	-0.0468
67	9.5	0.6420	0.9777	0.0116
68	11.6	0.9506	1.0645	0.4783
69	9.6	0.6667	0.9823	0.0408
70	9.3	0.5679	0.9685	-0.0762
71	9.7	0.6790	0.9868	0.0555
72	6.2	0.0864	0.7924	-1.0439
73	9.2	0.5309	0.9638	-0.1210
74	7.4	0.2469	0.8692	-0.5473
75	6.3	0.0988	0.7993	-0.9830
76	9.9	0.7407	0.9956	0.1303
77	9.6	0.6667	0.9823	0.0408
78	11.4	0.9383	1.0569	0.4448
79	9.5	0.6420	0.9777	0.0116
80	6.5	0.1235	0.8129	-0.8802

Table 2(b). Confidence intervals of breakdown voltage after 12000 h of aging

$\log \mathrm{Ln}\frac{1}{1-P}$	Log V_{inf}	Log V_{sup}
-1.9978	0.5451	0.6710
-1.2899	0.6962	0.7835
-0.9773	0.7627	0.8338
-0.7891	0.8031	0.8637
-0.6514	0.8321	0.8864
-0.5411	0.8553	0.9046
-0.4477	0.8747	0.9193
-0.3657	0.8914	0.9331
-0.2917	0.9063	0.9459
-0.2334	0.9210	0.9570
-0.1592	0.9338	0.9680
-0.0977	0.9459	0.9789
-0.0380	0.9578	0.9890
00.00	0.9648	0.9959
0.0806	0.9805	1.0104
0.1419	0.9921	1.0217
0.2067	1.0043	1.0345
0.2781	1.0172	1.0478
0.3622	1.0322	1.0647
0.4765	1.0522	1.0871
0.6632	1.0842	1.1253

b) Figure 2 shows the scatter diagrams of breakdown voltage before aging, and after 4000 h, 8000 h and 12000 h.

c) The values of V_0 and β, and the equations of Weibull plots are given in Tables 3-5. Some examples of Weibull graphs with confidence intervals are presented in Figures 3(a)-3(d). It is about virgin samples, and those aged after 4000 h, 8000 h, and 12000 h. The confidence intervals are marked with dashed lines.

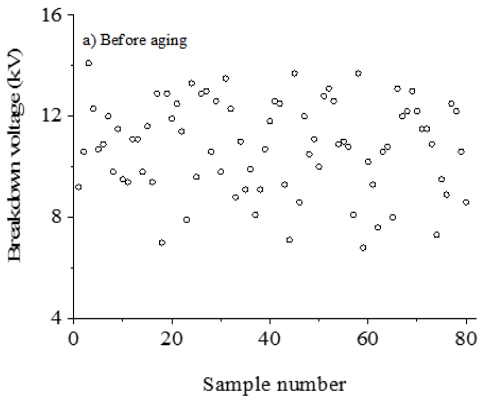

(a) Before aging

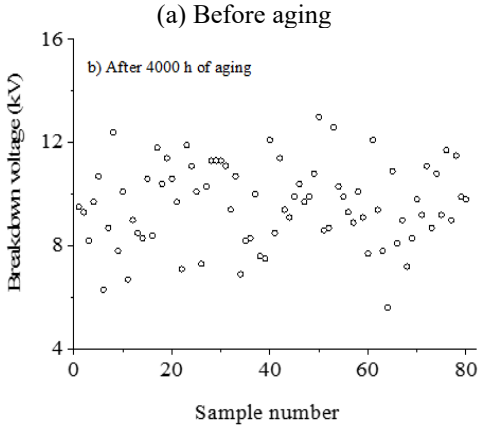

(b) After 4000 h of aging

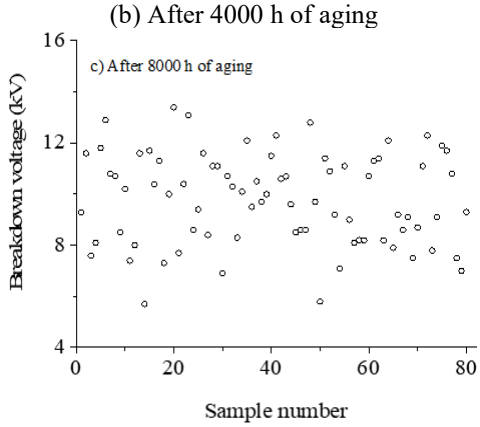

(c) After 8000 h of aging

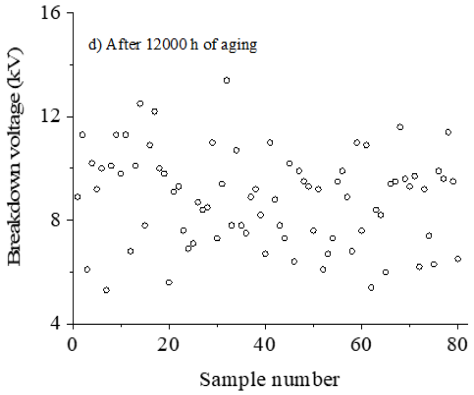

(d) After 12000 h of aging

Figure 2. Scatter diagram of breakdown voltage

Table 3. Values of V_0 and confidence intervals

Aging Time (h)	Breakdown Voltage (kV)
0	11.176 < V_0 = 11.489 < 11.807
500	10.030 < V_0 = 10.418 < 10.817
1000	10.748 < V_0 = 11.146 < 11.554
1500	9.136 < V_0 = 9.554 < 9.986
2000	9.433 < V_0 = 9.736 < 10.045
2500	9.449 < V_0 = 9.838 < 10.239
3000	10.465 < V_0 = 10.745 < 11.029
3500	9.974 < V_0 = 10.385 < 10.808
4000	9.967 < V_0 = 10.255 < 10.548
4500	10.217 < V_0 = 10.502 < 10.792
5000	9.843 < V_0 = 10.161 < 10.485
5500	9.439 < V_0 = 9.732 < 10.031
6000	9.858 < V_0 = 10.170 < 10.488
6500	10.290 < V_0 = 10.670 < 11.060
7000	9.807 < V_0 = 10.153 < 10.507
7500	9.974 < V_0 = 10.341 < 10.717
8000	10.196 < V_0 = 10.520 < 10.851
8500	10.137< V_0 = 10.491<10.854
9000	10.869 < V_0 = 11.187 < 11.510
9500	10.003 < V_0 = 10.313 < 10.609
10000	8.764 < V_0 = 9.099 < 9.443
10500	9.933 < V_0 = 10.178 < 10.426
11000	9.151 < V_0 = 9.444 < 9.743
11500	8.755 < V_0 = 9.163 < 9.607
12000	9.223 < V_0 = 9.561 < 9.907

Table 4. Values of β with confidence intervals

Aging Time (h)	Shape Parameter
0	6.054 < β = 7.179 < 8.220
500	4.404 < β = 5.222 < 5.979
1000	4.608 < β = 5.464 < 6.256
1500	3.742 < β = 4.437 < 5.080
2000	5.302 < β = 6.287 < 7.199
2500	4.146 < β = 4.917 < 5.630
3000	6.340 < β = 7.518 < 8.608
3500	4.146 < β = 4.917 < 5.630
4000	5.879 < β = 6.971 < 7.982
4500	6.076 < β = 7.205 < 8.250
5000	5.265 < β = 6.243 < 7.148
5500	5.475 < β = 6.492 < 7.433
6000	5.379 < β = 6.379 < 7.304
6500	4.613 < β = 5.470 < 6.263
7000	4.826 < β = 5.723 < 6.553
7500	4.630 < β = 5.490 < 6.286
8000	5.343 < β = 6.336 < 7.255
8500	4.869 < β = 5.774 < 6.611
9000	5.812 < β = 6.892 < 7.892
9500	5.659 < β = 6.711 < 7.684
10000	4.455 < β = 5.283 < 6.049
10500	6.874 < β = 8.151 < 9.333
11000	5.316 < β = 6.304 < 7.218
11500	3.500 < β = 4.151 < 4.753
12000	4.630 < β = 5.490 < 6.286

Table 5. Equations of Weibull graphs

Aging Time (h)	Equation of Weibull Plot
0	Y = 7.179 X – 7.612
500	Y = 5.222 X – 5.315
1000	Y = 5.464 X – 5.721
1500	Y = 4.437 X – 4.349
2000	Y = 6.287 X – 6.214
2500	Y = 4.917 X – 4.882
3000	Y = 7.518 X – 7.752
3500	Y = 4.917 X – 4.998
4000	Y = 6.971 X – 7.048
4500	Y = 7.205 X – 7.358
5000	Y = 6.243 X – 6.286
5500	Y = 6.492 X – 6.421
6000	Y = 6.379 X – 6.426
6500	Y = 5.470 X – 5.624
7000	Y = 5.723 X – 5.761
7500	Y = 5.490 X – 5.570
8000	Y = 6.336 X – 6.476
8500	Y = 5.774 X – 5.894
9000	Y = 6.892 X – 7.228
9500	Y = 6.711 X – 6.800
10000	Y = 5.283 X – 5.066
10500	Y = 8.151 X – 8.213
11000	Y = 6.304 X – 6.147
11500	Y = 4.151 X – 3.994
12000	Y = 5.521 X – 5.413

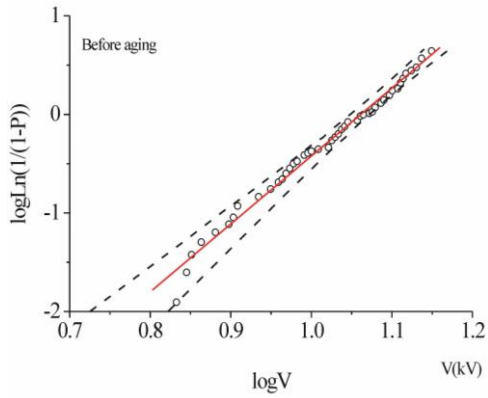

(a) Before aging: 11.176 < V_0 = 11.489 < 11.807; 6.054 < β = 7.179 < 8.220; Y = 7.179 X – 7.612

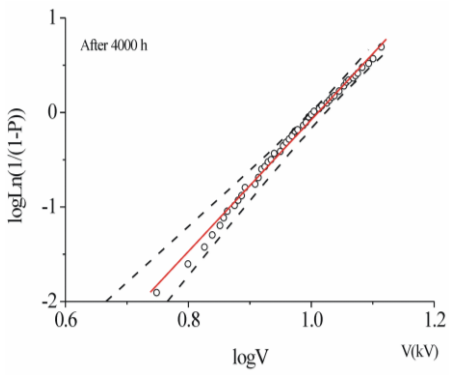

(b) After 4000 h: 9.967 < V_0 = 10.255 < 10.548; 5.879 < β = 6.971 < 7.982; Y = 6.971 X – 7.048

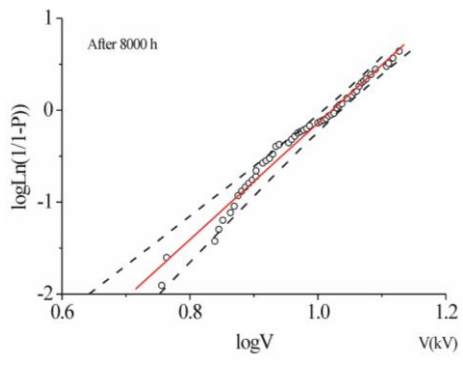

(c) After 8000 h: $10.196 < V_0 = 10.520 < 10.851$; $5.343 < \beta = 6.336 < 7.255$; $Y = 6.336\ X - 6.476$

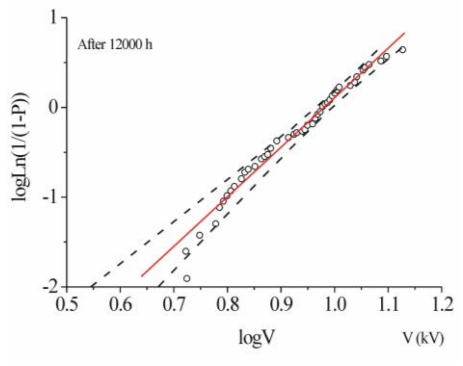

(d) After 12000 h: $9.223 < V_0 = 9.561 < 9.907$; $4.630 < \beta = 5.490 < 6.286$; $Y = 5.521\ X - 5.413$

Figure 3. Weibull plot of breakdown voltage

4.2 Variation of breakdown voltage versus aging time

Figure 4 displays breakdown voltage (V_0) against aging time. The curve shows a ragged variation with the attendance of several peaks. The variations can be depicted as follows:

- At the start of aging, V_0 decreases from 11.57 kV to 10.42 kV, raises to 11.15 kV and diminishes abruptly to 9.55 kV. Afterwards, V_0 increases to 10.75 kV and lowers to 10.25 kV corresponding to 4000 h.
- Beyond this time, V_0 increases a little to 10.50 kV and lessens until 9.75, then rises again to 10.67 kV. After it decreases to 10.10 kV, grows to 10.52 kV and remains somewhat constant until 8500 h.
- Last, V_0 augments to 11.19 kV and falls to 9.10 kV. After it increases to 10.18 kV and lessens again to 9.16 kV, then enlarges until 9.56 kV.

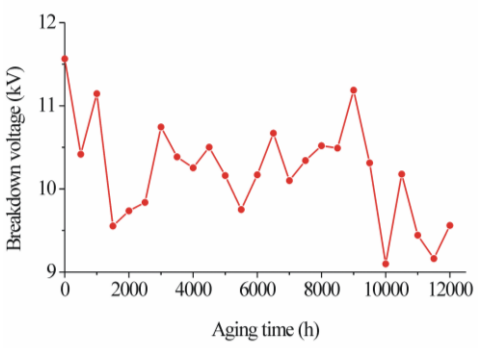

Figure 4. Breakdown voltage versus aging time

4.3 Variation of shape parameter in function of aging time

The variations of shape parameter (β) against aging time are represented in Figure 5 that shows, like Figure 4, an uneven evolution indicating several peaks. The evolutions can be summarized as follows:

- During the first 3000 h, β decreases from 7.18 to 5.22, rises to 5.94 and lessens again to 4.44 corresponding to 1500 h. Afterwards β increases to 6.29, decreases to 4.92 and grows until 7.52 after 3000 h.
- Later, it falls to 4.92, augments to 7.21 and lowers to 6.24 after 5000 h. Then it grows a little to 6.49, shortens to 5.47 and remains somewhat invariable until 7500 h.
- After this time, β increases to 6.34, decreases to 5.77 and raises to 6.89 corresponding to 9000 h. Afterwards β lessens to 5.28 and raises again reaching 8.15. Then, it drops until 4.15 and heightens to 5.52 for 12000 h.

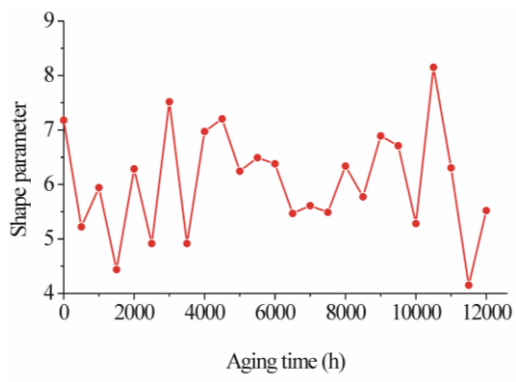

Figure 5. Shape parameter as a function of aging time

4.4 Infrared spectra

Table 6 shows the significant infrared absorbance bands of polyesterimide. The IR spectra, in the range 4000 cm^{-1} - 500 cm^{-1}, are presented in Figures 6-9.

Table 6. Absorbance bands

Absorbance Band Number	Wavenumber (cm^{-1})
1	3036
2	1774
3	1716
4	1701
5	1655
6	1486
7	1396

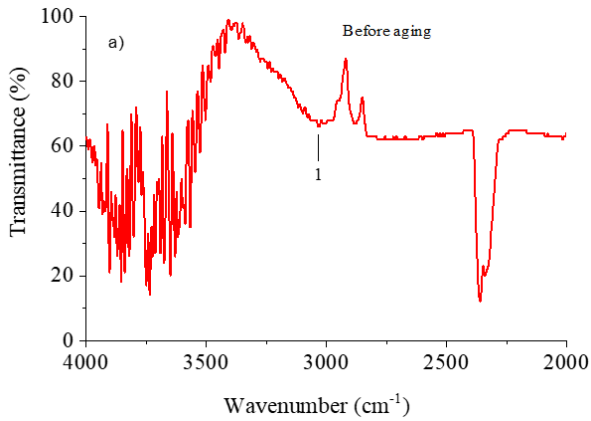

(a) Wavenumber between 4000 cm^{-1} to 2000 cm^{-1}

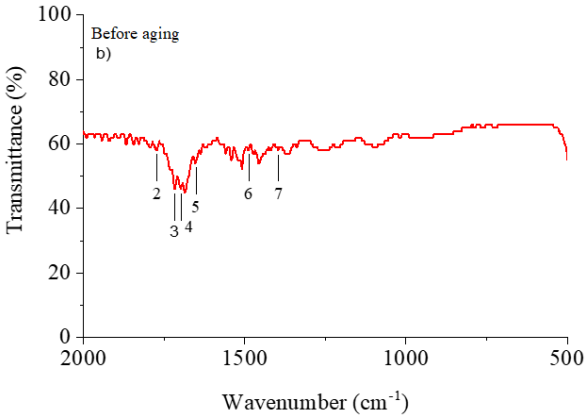

(b) Wavenumber between 2000 cm^{-1} to 500 cm^{-1}

Figure 6. FTIR spectrum before aging

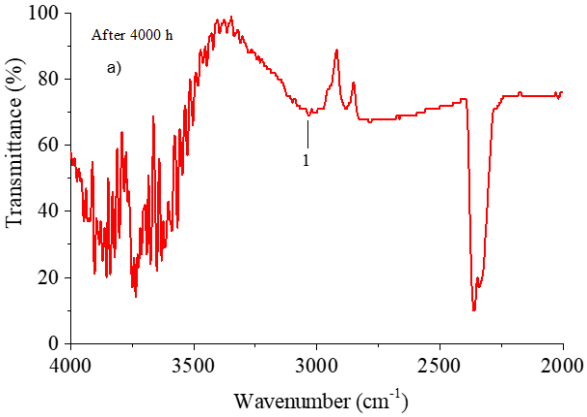

(a) Wavenumber between 4000 cm^{-1} to 2000 cm^{-1}

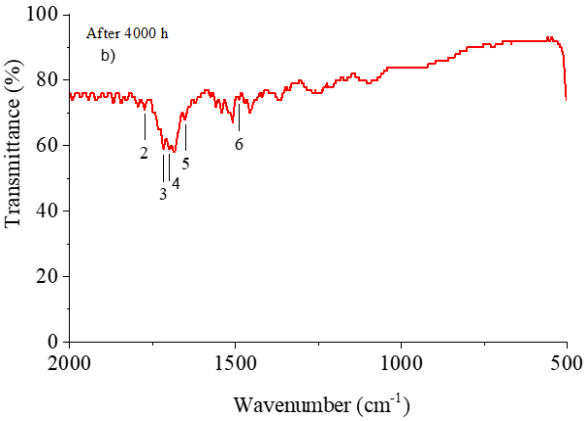

(b) Wavenumber between 2000 cm^{-1} to 500 cm^{-1}

Figure 7. FTIR spectrum after 4000 h

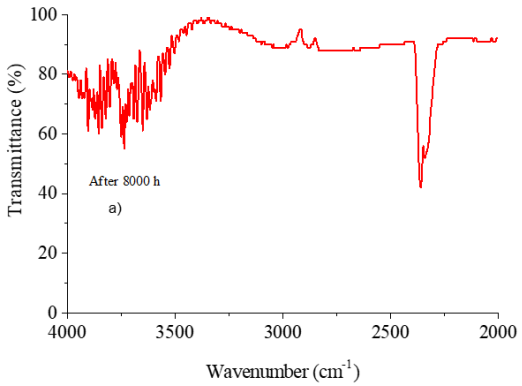

(a) Wavenumber between 4000 cm^{-1} to 2000 cm^{-1}

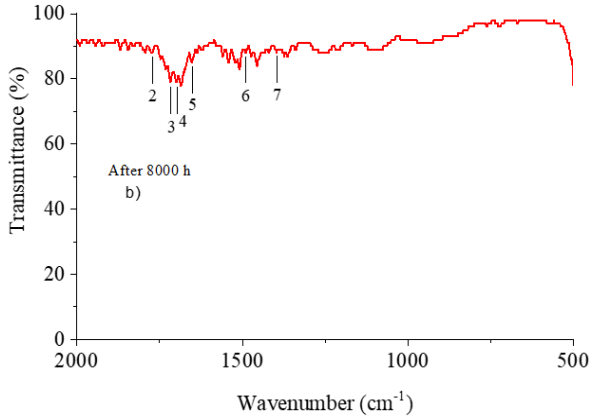

(b) Wavenumber between 2000 cm^{-1} to 500 cm^{-1}

Figure 8. FTIR spectrum after 8000 h

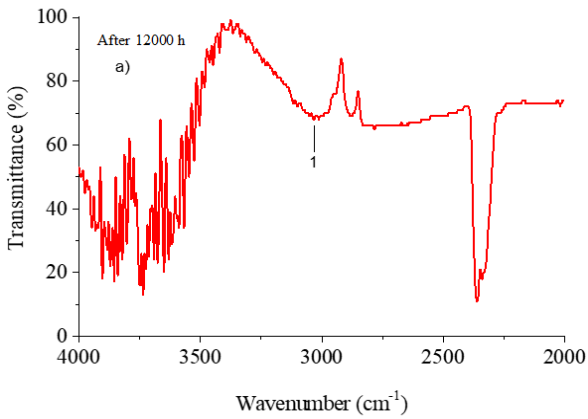

(a) Wavenumber between 4000 cm^{-1} to 2000 cm^{-1}

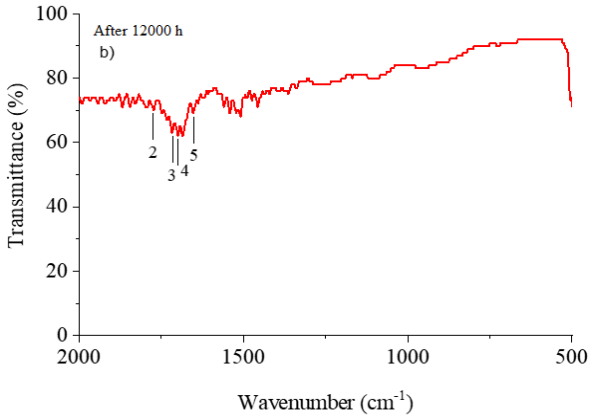

(b) Wavenumber between 2000 cm^{-1} to 500 cm^{-1}

Figure 9. FTIR spectrum after 12000 h

4.5 Discussion

1. After several hours of aging, water can diffuse into the polymer. Water plasticizes the material leading to the decrease of mechanical properties as ductility. This phenomenon has been reported by Merdas et al. [15].
2. The hydrolytic aging causes a lessening in viscosity expressing a weakening of molecular bonds and a raise in free volume. Therefore, the mean free path and the mobility of charge carriers enlarge inducing a reduction of breakdown voltage. While the increase of the breakdown voltage is due to the arrangement in the structure producing, in the contrary, a shortening of mean free path and the mobility of charge carriers. The

maximum variation of V_0 is 21.34%.

3. The breakdown voltage is linked to the presence of defects which can be voids, metallic inclusions, electrode asperities and laminations at the electrode-polymer interface. These defects can exist within the insulations during the manufacturing or created by the hydrolytic aging.
4. As it can be shown, the dispersion of data alters from a distribution to another.
5. The change of β is assigned to the size distribution of defects. The reduction is ascribed to the size raise of defects. On the other hand, the increase is due to the arrangement in the molecular structure. The maximum variation β is 42.20%.
6. The dielectric breakdown of polymeric materials is related to the presence of space charge as indicated by Chen et al. [16]. Indeed, in the present work, the average maximum value of electrical field is about 100 kV/mm and the space charge can be shaped due to the injection of electrons/holes from the conductors (electrodes).
7. The interpretation of FTIR spectra is presented as follows:

a) Before aging

It arises an absorbance band at 3036 cm^{-1} allotted to the stretching vibration of hydroxyl groups (OH) [17]. We notice two absorption peaks at 1774 and 1716 cm^{-1} attributed to the asymmetrical stretching vibration and symmetrical stretching vibration of carbonyl (C=O) on the imide ring, respectively [18]. The absorbance band, detected at 1701 cm^{-1}, matches to the C=O vibration of ester groups [19, 20]. The absorbance band at 1655 cm^{-1} corresponds to stretching vibration on the C=O ester bond [18]. The absorbance band at 1486 cm^{-1} is allotted to C-C stretching vibration on benzene ring skeleton [18]. The C-N stretching vibration of aromatic-imide is shown at 1396 cm^{-1} [18].

b) After aging, we remark a change of the spectra. The absorbance band at 1396 cm^{-1} disappears after 4000 h. After 8000 h, the vanishing of the absorbance band at 3036 cm^{-1} is noted. After 12000 h, we notice the disappearance of two absorbance bands at 1486 and 1396 cm^{-1}.

8. Depending on the investigation yielded by Araki and Taguchi [21], copper was detected in the polyesterimide layer. Oxygen can easily diffuse into the polyesterimide and attack the copper leading to formation of copper oxide. This latter grows into the insulation. The formation and the growth of copper oxide was confirmed by Lukas Korcak and Culliton [22]. The degradation of polyesterimide is a result of scission reaction of imide bond and ester bond at the copper – polyesterimide interface. The dissolution of copper can accelerate the decomposition of the polymer.
9. In a previous work, we studied the influence of hydrolytic aging on breakdown voltage of wire enameled including two layers of insulations [23]. The samples are twisted pair copper conductor insulated by polyesterimide (class H) covered with a film of polyamide imide (class C). By comparing the results obtained in the preceding work and the present study, we can conclude that:
   - Before aging, the breakdown voltage is 12.709 kV in the precedent study. On the other hand, its value is 11.489 kV in the actual work. Therefore, the breakdown voltage is greater in the prior work; that is a difference of 9.6%.
   - After a same aging time, the breakdown voltage corresponding to the current work is higher than that matching to the anterior investigation. The difference attains 36.58%.
   - In the antecedent work, the degradation did not occur after 15000 h of aging. On the contrary, in the actual work, the degradation takes place after 12000 h.

5. CONCLUSIONS

The next points can be taken from this investigation:

1. The breakdown voltage of polyesterimide is modified by hydrolytic aging. The increase is assigned to the arrangement in the structure of the polymer. Whereas its shortening is attributed to the growth in the free volume leading to the raise in the mean free path. Thereby the mobility of charge carriers augments.
2. The shape parameter varies against aging time. The raise is ascribed to the arrangement in the molecular structure. While the shortening is allotted to the heightening in the sizes of defects.
3. The breakdown voltage depends on the accumulated space charge. This latter is due to the injection of electrons\holes from the conductors within the insulation.
4. The FTIR shows a modification of the spectra after aging resulting to the degradation of the insulating material. It is about the vanishing of absorbance bands at 3036 cm^{-1} after 8000 h, 1486 cm^{-1} and 1396 cm^{-1} after 12000 h, and 1396 cm^{-1} after 4000 h.
5. At long term of aging, decomposition of imide bond and ester bond take place leading to the degradation of the insulating material. The degradation is expedited by the dissolution of copper producing a copper oxide.
6. We notice that, after a given aging time, the breakdown voltage of the insulation is more significant than that in a prior work. Further, in the preceding investigation, the degradation of the dielectric material did not happen.

REFERENCES

[1] Farahani, M., Borsi, H., Gockenbach, E. (2006). Dielectric response studies on insulating system of high voltage rotating machines. IEEE Transactions on Dielectrics and Electrical Insulation, 13(1): 383-393. http://doi.org/10.1109/TDEI.2006.1624283

[2] Kavanagh, D.F., Gyftakis, K.N., McCulloch, M.D. (2019). Early-onset degradation of thin-film magnet wire insulation for electromechanical energy converters. In the 12th International Symposium on Diagnostics for Electrical Machines, Power Electronics and Drives, Toulouse, France, pp. 37-43. http://doi.org/10.1109/DEMPED.2019.8864916

[3] Grubic, S., Aller, J.M., Lu, B., Habetler, T.G. (2008). A survey on testing and monitoring methods for stator insulation systems of low-voltage induction machines focusing on turn insulation problems. IEEE Transactions

on Industrial Electronics, 55(12): 4127-4136. https://doi.org/10.1109/TIE.2008.2004665

[4] Ksouri, I, Almeida, O.D., Haddar, N. (2017). Long term ageing of polyamide 6 and polyamide 6 reinforced with 30% of glass fibers: Physicochemical, mechanical and morphological characterization. Journal of Polymer Research, 24: 133. https://doi.org/10.1007/s10965-017-1292-6

[5] Ji, Y., Giangrande, P., Zhao, W., Madonna, V., Zhang, H., Li, J., Galea, M. (2023). Investigation on combined effect of humidity-temperature on partial discharge through dielectric performance evaluation. IET Science, Measurement & Technology, 17: 37-46. https://doi.org/10.1049/smt2.12128

[6] Brandes, H., Hillmer, T., Frost, N., Mesrobian, A. (2006). Class H insulation system for rotating equipment. In Conference Record of the 2006 IEEE International Symposium on Electrical Insulation, Toronto, ON, Canada, pp. 346-349. https://doi.org/10.1109/ELINSL.2006.1665329

[7] Arikan, O., Uydur, C.H.C., Kumru, C.F. (2022). Prediction of dielectric parameters of an aged MV cable. A comparison of curve fitting, decision tree and artificial neural network methods. Electric Power Systems Research, 208(6): 107892. http://doi.org/10.1016/j.epsr.2022.107892

[8] Havran, P., Cimbala, R., Kurimsky, J., Dolnik, B., Kolcunova, I., Medved, D., Kiraly, J., Kohan, V., Sarpataky, L. (2022). Dielectric properties of electrical insulating liquids for high voltage electric devices in a time-varying electric field. Energies, 15(1): 391. http://doi.org/10.3390/en15010391

[9] Lian, Z., Niu, H., Li, S. (2019). Detection of ageing effect in polyesterimide by terahertz time-domain spectroscopy. IEEE Transactions on Terahertz Science and Technology, 9(6): 651-658. https://doi.org/10.1109/TTHZ.2019.2941125

[10] Niu, H., Liu, W., Chi, X., et al. (2018). Effects of hygrothermal ageing on breakdown performance of polyesterimide nanocomposites. In 2018 Condition Monitoring and Diagnosis (CMD), Perth, WA, Australia, pp. 1-5. https://doi.org/10.1109/CMD.2018.8535812

[11] Nedjar, M. (2013). Statistical study in short-term dielectric breakdown of polyvinyl chloride. Journal of Vinyl and Additive Technology, 19(3): 177-182. https://doi.org/10.1002/vnl.21312

[12] Lai, C.D. (2014). Generalized Weibull Distributions. Springer, Berlin, Heidelberg, pp. 23-75. https://doi.org/10.1007/978-3-642-39106-4

[13] Chauvet, C., Laurent, C. (1993). Weibull statistics in short-term dielectric breakdown of thin polyethylene films. IEEE Transactions on Electrical Insulation, 28(1): 18-29. http://doi.org/10.1109/14.192236

[14] Raju, G., Katebian, A., Jafri, S.Z. (2001). Application of Weibull distribution for high temperature breakdown data. In 2001 Annual Report Conference on Electrical Insulation and Dielectric Phenomena (Cat. No. 01CH37225), Kitchener, ON, Canada, pp. 173-176. https://doi.org/10.1109/CEIDP.2001.963514

[15] Merdas, I., Thominette, F., Verdu, J. (2000). Humid aging of polyetherimide. II. Consequences of water absorption on thermomechanical properties. Journal of Applied Polymer Science, 77(7): 1445-1451. http://doi.org/10.1002/1097-4628(20000815)77:73.3.CO;2-E

[16] Chen, G., Zhou, C., Li, S., Zhong, L. (2016). Space charge and its role in electric breakdown of solid insulation. In the International Power Modulator and High Voltage Conference, San Francisco, CA, USA, pp. 120-127. http://doi.org/10.1109/IPMHVC.2016.8012888

[17] Žagar, E., Grdadolnik, J. (2003). An infrared spectroscopic study of H-bond network in hyperbranched polyester polyol. Journal of Molecular Structure, 658(3): 143-152. https://doi.org/10.1016/S0022-2860(03)00286-2

[18] Qi, C., Yang, W., He, F., Yao, J. (2020). The thermal properties and degradability of chiral polyester-imides based on several L/D-Amino acids. Polymers, 12(9): 2053. https://doi.org/10.3390/polym12092053

[19] Fetouhi, L., Martinez-Vega, J., Petitgas, B. (2018). Electric conductivity, aging and chemical degradation of polyesterimide resins used the impregnation of rotating machines, IEEE Transactions on Dielectrics and Electrical Insulation, 25(1): 294-305. http://doi.org/10.1109/TDEI.2018.006823

[20] Calabrese, E., Raimondo, M., Catauro, M., et al. (2023). Thermal and electrical characterization of polyester resins suitable for electric motor insulation. Polymers, 15(6): 1374. https://doi.org/10.3390/polym15061374

[21] Araki, C., Taguchi, T. (1993). Thermal degradation of polyesterimide magnet wire. In the IEEE Conference of Electrical Insulation and Dielectric Phenomena (CEIDP'93), Pocono Manor, PA, USA, pp. 526-531. https://doi.org/10.1109/CEIDP.1993.378919

[22] Lukas Korcak, L., Culliton, D. (2021). Copper oxide formations under polymer coatings during accelerated thermal aging. In 2021 4th International Conference on Electronics and Electrical Engineering Technology, Nanjing, China, pp. 64-68. http://doi.org/10.1145/3508297.3508376

[23] Kerkarine, F., Nedjar, M. (2024). Hydrolytic aging of wire enameled with polyesterimide and polyamide imide used in electrical machines. Mathematical Modelling of Engineering Problems, 11(4): 1053-1059. https://doi.org/10.18280/mmep.110423